Arch Virol (2003) 148: 723–744
DOI 10.1007/s00705-002-0949-5

Archives of Virology
Printed in Austria

Characterization of the RNA-binding activity of VP3, a major structural protein of *Infectious bursal disease virus*

G. Kochan, D. Gonzalez, and **J. F. Rodriguez**

Departamento de Biología Molecular y Celular, Centro Nacional de Biotecnología, CSIC, Campus Universidad Autónoma de Madrid, Madrid, Spain

Received August 23, 2002; accepted October 30, 2002
Published online January 16, 2003

Summary. *Infectious bursal disease virus* (IBDV) is the agent of an immune-depressive disease affecting the poultry industry worldwide. Infection of IBDV leads to expression of five mature virus-encoded proteins. Proteolytic processing of the virus-encoded polyprotein generates VP3 which coats the inner surface of the IBDV capsid. In this report, we describe the characterization of the RNA-binding activity of VP3. For these studies, the VP3 coding region was fused to a histidine tag and expressed in insect cells using a recombinant baculovirus. The histidine-tagged VP3 was affinity-purified and used to study its ability to bind RNA molecules using three complementary methods: (i) Northwestern blotting; (ii) binding of VP3 protein-RNA complexes to nitrocellulose membranes; and (iii) electrophoretic mobility shift assays. The results demonstrated that VP3 efficiently bound ssRNA and dsRNA. Under the experimental conditions used in this study, the formation of VP3-RNA complexes did not depend upon the presence of specific RNA sequences. A series of histidine-tagged VP3 deletion mutants spanning the whole VP3 coding region were generated. The use of these mutants revealed that the VP3 RNA-binding domain layed in a highly conserved 69 aa stretch close to the N-terminus of the protein.

Introduction

Infectious bursal disease virus (IBDV) is the type species of the genus *Avibirnavirus* of the family *Birnaviridae* [27]. Infection of young chickens with IBDV leads to infectious bursal disease (IBD), characterized by the destruction of the bursa of Fabricious that results in a severe immunosuppression. IBD causes major economical losses to the poultry industry [34, 39] and it might also affect several species of wild birds [18, 35, 45].

IBDV virions are non-enveloped, possess a single protein shell and present a diameter of 65–70 nm. The capsid, with icosaedral symmetry, consists of 780 subunits clustered as 260 outer trimers arranged with a triangulation number T = 13 [6, 9]. IBDV contains a dsRNA genome formed by two segments, segment A, (3.2 kb), and segment B (2.9 kb) [13, 24, 32]. Segment A contains two partially overlapping open reading frames (ORF 1 and ORF 2). ORF 1 encodes the nonstructural protein VP5 (17 kDa), important for virus egress [29, 46]. ORF 2 encodes a 110 kDa polyprotein that is autoproteolitically processed into VPX (48 kDa), VP4 (28 kDa) and VP3 (32 kDa). VPX is further processed to render VP2 (41 kDa) [10, 11, 40]. VPX, VP2 and VP3 are the major structural proteins [9], while VP4 is the viral protease responsible for polyprotein processing [4].

Segment B encodes VP1, the putative viral RNA-dependent RNA polymerase (RdRp) [7, 30]. In mature virions VP1 is complexed to the dsRNA segments and interacts with VP3 [25, 28, 43]. VP2 forms trimers that build the external capsid surface, and VP3 is coating the internal surface of the particle [9]. According to previous experimental data, VP3 might interact with the virus genome [22, 23]. Cryoelectron microscopy images of IBDV virus-like particles (VLPs), generated by polyprotein expression using a recombinant vaccinia virus, strongly suggested the presence of packaged nucleic acid (J. R. Castón, personal communication). Since VLPs do not contain VP1, VP3 is the most likely candidate for unspecific encapsidation of nucleic acids.

Studies carried out with *Infectious pancreatic necrosis virus* (IPNV), the type species of the genus *Aquabirnavirus* of the family *Birnaviridae* [27], led to the isolation of ribonucleoprotein complexes from disrupted IPNV virions [22]. These complexes were shown to contain VP3 and RNA. However, it was not determined whether VP3 directly bound to RNA molecules or to VP1 complexed to dsRNA [22]. VP3-RNA complexes were also purified from supernatants of IPNV-infected cell cultures, although the nature of the bound RNA was not determined [23].

The main goal of this work was to carry out a systematic analysis to ascertain the capability of IBDV VP3 to bind RNA in the absence of other virus-encoded proteins. The positive results obtained led us to continue our investigation in order to map the VP3 RNA-binding domain.

Materials and methods

Cells and viruses

African green monkey kidney epithelial cells (BSC40) were grown in Dulbecco modified Eagle's medium (DMEM) containing 10% newborn calf serum (NCS). The IBDV Soroa strain was grown and titrated as described [16].

Trichoplusia Ni H5 cells (Invitrogen) were grown in monolayers at 28 °C in TC100 medium (Gibco BRL) supplemented with 10% fetal calf serum. Recombinant baculoviruses (rBVs) were generated using the Bac-to-Bac system (Gibco BRL). Generation, growth, and titration of rBVs were carried out as described by the manufacturer.

Generation of VP3 deletion mutants and recombinant baculoviruses

IBDV VP3 coding sequence, corresponding to polyprotein aa positions 756 to 1012, was subcloned from plasmid pVOTE1/POLY [16] into the pFastBac HTc vector (Gibco BRL). Briefly, pVOTE1/POLY cDNA was digested with *Bam*HI and partially with *Nco*I, and the resulting DNA fragment containing the VP3 gene was ligated to plasmid pFastBac HTc restricted with the same enzymes, generating the plasmid pFastBac-VP3-His. This plasmid contained the VP3 gene fused to a histidine tag under the control of the polyhedrin promoter.

VP3 deletion mutants were generated by overlap extension PCR [36] using synthetic primers containing the desired deletions and using the pcDNA3-POLY plasmid [40] as a template. PCR products were obtained either with primer A (5′-GCGCGAGCTCCGTTTCCCTC ACAATCCACGCGAC-3′) with the corresponding reverse-sense primer (Table 1) or with primer B (5′-GCGCGGATCCTCATCCAAGGTCCTCATC AGAGACA-3′) with the corresponding reverse-sense primer (Table 1). Both products were recombined by PCR using primers A and B. PCR products were digested with *BamH*I and *Xho*I and cloned into the pFastBac-VP3-His plasmid restricted with the same enzymes. In this way, a series of VP3 mutants containing small deletions ($\approx$ 75 bp) spanning the whole coding region of the protein was generated (Table 1). The carboxy-terminal deletion mutants VP3Δ1008–1012 (numbers represent positions of aminoacids in the polyprotein, flanking the deletions) and VP3Δ971–1012 presenting deletions of 5 and 42 residues, respectively, were obtained by cloning the VP3 fragment resulting from digestion with *Xba*I and *Not*I from plasmids pcDNA3-VP3Δ1008–1012 and pcDNA3-VP3Δ971–1012 (Maraver et al., submitted), respectively, into the pFastBact-HTc vector. All constructs were sequenced to confirm the mutations.

Preparation of RNA and DNA probes

To study VP3 RNA-binding activity, different [$\propto$-^{32}P]-labeled single-stranded RNA (ssRNA) probes, containing viral and non-viral sequences, were generated using the Ribo-Max kit (Promega). Briefly, transcription reactions were carried out by the T7 RNA polymerase for 4 h at 37 °C. Radioactive labeling was introduced including 10 μCi[$\propto$-^{32}P]ATP (3000 Ci/mmol) in transcription reactions (20 μl final volume). Synthesized RNAs were purified using MicroSpin columns S-200HR (Amersham Pharmacia Biotech). Two IBDV virus-derived ssRNA probes were produced, probes A and B. RNA probe A (3040 nt) was synthesized from IBDV ORF A2 by transcription from the plasmid pcDNA-POLY [40] linearized with *Sma*I. The sequence of ssRNA probe A corresponded to IBDV polyprotein coding region. RNA probe B (186 nt) contained the 5′ first 152 nt fused to the 3′ 34 nt non-coding regions (UTRs) from segment B. This probe was produced using the plasmid TV2-5′3′ (Maraver et al., submitted for publication) linearized with *Sma*I.

Two non-viral ssRNA probes, GFP and PL, were also produced as described above. RNA probe GFP (1300 nt) was obtained from green fluorescent protein (GFP) mRNA fused to the encephalomyocarditis virus (EMCV) leader sequence. This probe was produced by *in vitro* transcription using as a template the pVOTE2-GFP plasmid restricted with *Pst*I and Klenow-treated. Plasmid pVOTE2-GFP was obtained by blunt-end ligation of plasmid pVOTE-1 [44] restricted with *Dra*I and *Sma*I, and the GFP gene excised by *Not*I digestion from the Green Lantern plasmid (Gibco BRL) followed by treatment with Klenow. RNA probe PL (100 nt), was obtained by run off transcription of the polylinker region of the pcDNA3 plasmid (Promega) linearized with *Xba*I. The purity of all synthesized ssRNA probes was confirmed by polyacrylamide gel electrophoresis under denaturing conditions and detection by autoradiography. The concentration of RNA preparations was estimated by either electrophoresis in polyacrylamide or agarose gels and ethidium bromide staining or

Table 1. Synthetic oligonucleotides used for generation of VP3 deletion mutants

Mutant	Virus sense primer (5′-3′) (sp)	Reverse sense primer (5′-3′) (rp)	Restriction sites
Δ756–780	CCGCGAATTCCTATTCCAATCTGCACTCAGT		*EcoR*I
Δ781–807	GCAGCAGCCAACGTGGACCCAG	CGCATCCGATGGGCGTTCGGGT	a
	ACCCAAACGCCCATCGGATGCG	CTGGGTCCACGTTGGCTGCTGC	
Δ808–832	CATGGCCAACTTCGCACTCAGCT	CCACTCCGTAGCCTGCTGTCCC	a
	ACGGGACAGCAGGCTACGGAGTGG	GTAGCTGAGTGCGAAGTTGGCCATG	
Δ833–855	GCAAGTCGCAAAGGGCCAAGAC	CCATCTTTTTGAGATCCGTGTCT	a
	ACGGATCTCAAAGAAGATGG	TGGCCCTTTGCGACTTGC	
Δ856–879	GGAAGCACAGAGGGAAAAAGA	GGCCTGGGCTTGGCCCTCGGTG	a
	CCACCGAGGGCCAAGCCCAGGCC	GTCTTTTTCCCTCTGTGCTTCC	
Δ880–905	GAATGGGTAGCACTCAATGGGG	GCTCTTCTCTGCATGCACGTAG	a
	ACTACGTGCATGCAGAGAAGAGC	TCCCCATTGAGTGCTACCCATTC	
Δ906–930	CCGGACCCAAACGAGGACTATC	GGGGTGGCTCTGCCTGTCCTGG	a
	TAGCTCCAGGACAGGCAGAGCCACCCC	AGCTAGATAGTCCTCGTTTGGGTCCGG	
Δ931–955	GGGCAGCTACGTCGATCTACGG	CATCTGTTCTTGGTTTGGGCCC	a
	GGGCCCAAACCAAGAACAGATG	CCGTAGATCGACGTAGCTGCCC	
Δ956–979	GTCTATGAAATCAACCATGGAC	GGCTTGGGCTTTGGTAGAGCAC	a
	GTGCTCTACCAAAGCCCAAGCC	GTCCATGGTTGATTTCATAGAC	

a, no restriction sites were introduced

determination of the absorbance at 260/280 nm. The specific activity of radioactively labeled RNA probes was determined by scintillation counting.

For binding studies to double-stranded IBDV RNAs (dsRNAs), virus dsRNA was purified from BSC40 cells infected with IBDV using the Ultraspect RNA extraction reagent kit (Biotecx laboratories, Inc.) following the instructions provided by the manufacturer. Subsequently, IBDV dsRNA segments A and B were separated in 1% agarose gels, and segment A was purified using RNaid kit (Q. Biogene). Plasmid DNA pcDNA3 linearized with *Sma*I was used as double-stranded DNA (dsDNA) competitor probe. Single-stranded DNA from PhiX phage virus (Biolabs) was used as ssDNA competitor probe.

Expression and purification of wild-type (WT) and mutant VP3 proteins

WT and mutant VP3 proteins were expressed using a baculovirus-based expression system. Briefly, a 150 mm diameter culture plate of confluent H5 insect cells were infected with rBVs at a multiplicity of infection (moi) of 1. Infected cells were harvested at 72 hpi and lysed on ice with a Dounce homogenizer in TNN buffer (50 mM Tris, 500 mM NaCl, and 0.1% NP-40, pH 7.5) in the presence of protease inhibitors (Complete Mini, Roche). Cell lysates were clarified by centrifugation at 1000 X g for 10 min at 4 °C. Recombinant proteins were purified from the resulting supernatants using a Ni-His trap affinity column (Pharmacia LKB) following the instructions provided by the manufacturers. The expressed proteins were eluted from the column with a continuous imidazol gradient from 4 mM to 600 mM. His-tagged WT VP3 protein was eluted at an imidazol concentration of 500 mM. For elution of each VP3 deletion mutant, imidazol concentrations were optimized. The purity of eluted proteins was assessed by SDS-PAGE analysis and Coomassie staining. The concentration of purified proteins was estimated using the BCA system (Pierce).

To confirm the identity of baculovirus-expressed VP3 proteins, Western blot analyses were carried out from infected cell lysates as described [17]. Briefly, after separation of the cellular proteins by SDS-PAGE and transfer onto nitrocellulose membranes, filters were saturated with 5% non-fat dried milk in PBS for 1 h at room temperature (RT), followed by incubation with specific anti-VP3 monoclonal (MAb) or polyclonal antibodies [17] diluted 1:1000 in blocking solution. Excess of unbound antibodies was removed by washing three times in PBS buffer. After washing, horseradish peroxidase-conjugated secondary goat-anti rabbit MAb or rabbit anti-mouse MAb (Cappel) were added in blocking solution (1:1000 dilution) and incubated for 1 h at RT. After removing the unbound conjugates, membranes were developed in PBS containing 0.02% 1-chloro-4-naphtol and 0.006% hydrogen peroxide. After developing, membranes were washed in distilled water and dried.

Characterization of VP3 ssRNA-binding activity by Northwestern blot analysis

Northwestern blot assays were carried out with cellular extracts from cells infected with WT or rBVs as described [19]. Infected cells were collected at 72 hpi and pelleted by centrifugation at 400 X g for 5 min at 4 °C. Cell pellets were washed with PBS and lysed in TNN buffer by incubation on ice for 10 min with frequent and intensive vortexing. After cell lysis, cellular extracts were mixed (1:1) with loading buffer (16% glycerol, 0.2% SDS, 2 mM DTT, 0.2% bromophenol blue, 24 mM Tris, pH 6.8 in PBS). Samples were incubated at 37 °C for 10 min with gentle agitation and centrifuged at 1000 X g for 5 min at RT to remove cell debris. In all cases 100 μg of cellular extracts from cells infected either with WT BV or rBV expressing VP3 (VP3-Bac) was separated in 12% SDS-PAGE gels and transferred onto nitrocellulose filters in Tris-glycine buffer (25 mM Tris, 192 mM glycine, pH 8.3). Filters were incubated 16 h at 4 °C in renaturing buffer (50 mM NaCl, 1 mM EDTA, 0.02% Ficoll, 0.02% bovine serum albumin (BSA), 0.02% polyvinylopirolidone, 0.1% Triton X-100, 10 mM Tris, pH 7.5). Afterwards,

membranes were incubated in 10 ml of renaturing buffer containing 10^6 cpm of ^{32}P-labeled probe B (0.5 ng/ml) in the presence of an excess (10^4 ng/ml) of yeast whole RNA over labeled probe. After incubation for 2 h, membranes were washed four times with renaturing buffer for an additional hour to remove unbound probe. After drying, membranes were analyzed with a phosphorimager (STORM 860, Molecular Dynamics). The same membranes were processed for Western blot using specific anti-VP3 antibodies. Experiments were repeated three times with independent preparations of cell extracts.

Characterization of the VP3-ssRNA interaction by binding of VP3-RNA complexes to nitrocellulose membranes

To characterize the VP3 ssRNA-binding activity, a filter-binding assay was performed as described [21]. The affinity of VP3 protein to ssRNA was estimated from three independent experiments using ^{32}P-labeled virus ssRNA probes. Briefly, increasing amounts (from 5×10^{-2} mM to 5×10^{-6} mM) of purified VP3 or BSA, used as a control for non-specific interaction, were mixed with 10^6 cpm of ^{32}P-labeled ssRNA probe B (5×10^{-6} mM) in binding reaction buffer (50 mM Tris, 150 mM KCl, 150 mM NaCl 10% Glycerol, 0,01% Triton X 100), in 16 µl final volume, so the VP3/RNA molar ratio in these experiments varied from 10^4 to 1. Binding reaction mixtures were incubated at RT for 1 h and filtered through nitrocellulose membranes using a dot-blot apparatus. In order to always use the same protein/RNA ratio, when other probes were used the amount of the probes were corrected according to their size. The proportion of the retained probe in the filters was quantified by densitometry using a phosphorimager apparatus. A VP3-RNA binding curve was drawn by plotting the percentage of retained radioactivity as a function of VP3 protein concentration. Assuming that the plateau reached represented the complete binding of the RNA, the apparent Kd corresponded to the concentration of VP3 protein required to reach half saturation [21]. Kd estimation was performed assuming a simple molecule-to-molecule binding equilibrium reaction.

To transform the non-linear curve observed for VP3-RNA binding to linear, a Hill plot was obtained as described [3, 5], by plotting Log [retained radioactivity/(100-retained radioactivity)] as a function of Log (VP3 concentration). For the Hill plot analysis, means of retained radioactivity from three independent experiments were used. A linear regression was performed by the least squares procedure (9 degrees of freedom) and the associated probability to the correlation coefficient (R) was calculated obtaining a t value for a t-Student test, as described [37]. The Hill coefficient (n_H) was obtained as the slope of the regression line and the $K_{0.5}$ value (amount of VP3 concentration to give half saturation, apparent Kd) was calculated [3].

Competition assays based on nitrocellulose binding were carried out using virus-derived radiolabeled ssRNA probes together with increasing concentrations of non-radioactive competitor RNA and DNA probes. Briefly, VP3-RNA binding reactions were carried out as described above using radiolabeled ssRNA probes B and A. Binding reactions were performed in the presence of increasing concentrations, molar ratios of 1:1, 1:10, 1:100 and 1:1000, of competitor unlabeled RNA or DNA probes. Reaction mixtures were filtered through nitrocellulose membranes, and the retained radioactivity was quantified as described above. Competition experiments were also repeated three times to obtain representative means.

Characterization of VP3 ssRNA-binding activity by electrophoretic mobility shift assays (EMSA)

The interaction of VP3 with ssRNA was analyzed by EMSA as described [1, 5] with minor modifications. Briefly, VP3-ssRNA complexes were allowed to form using increasing amounts

of purified VP3 as described above. After incubation, aliquots of the reaction mixtures were loaded onto 7% polyacrylamide gel in TBE buffer (45 mM Tris-borate, 1 mM EDTA, pH 8.0), and gels were run in TBE buffer at 4 °C. Gels were dried and exposed using a phophorimager apparatus. Excess of BSA (from 1 to 10 mM) was used as a non-specific protein in RNA-binding reactions. For supershift assays, after a 20 min incubation at RT, the reaction mixtures were supplemented with 1 μg of either VP3-specific monoclonal antibodies (MAbs) or non-specific antibodies (preimmune mouse IgG) and maintained for 1 h at RT. Thereafter, reaction mixtures were resolved in polyacrylamide gels and VP3-ssRNA complexes were revealed as described above. Experiments were repeated three times.

Alignment of VP3 protein sequences

To find the level of sequence conservation of the VP3 ssRNA-binding domain among different birnaviruses, known VP3 sequences from representative members of the family were aligned and compared using the Clustal algorithm [41]. For alignment conditions, the table of residue weights used was PAM250 with a gap penalty of 10 [12]. For this purpose, the sequences of VP3 proteins from different species belonging to the avibirnavirus, aquabirnavirus, and entomobirnavirus genera as well as to unclassified birnaviruses were retrived from GeneBank. For genus avibirnavirus, IBDV virus serotype 1, strain Soroa (AF140705.1), strain OH (U30818.1), strain STC (D00499), Cu-1wt virus (AF362747.1), and serotype 2 (AF362773.1) were used. For aquabirnavirus genus, VP3 sequences from IPNV strains DRT (D26526.1), Jasper (NC_001915), SP (AF342728.1), and N1 (D00701) were used. In the case of genus entomobirnavirus, the VP3 protein sequence from Drosophila X virus (U60650) was used. For unclassified birnaviruses, the species marine birnavirus (AB006783) and yellowtale ascites virus (AB011440.1) were used.

Results

Previous studies performed with the aquabirnavirus IPNV had shown the presence of VP3 in ribonucleoprotein complexes isolated from virus particles [22]. This observation along with the fact that VP3 coats the inner surface of the virus particle [6, 9] suggested the possibility that VP3 might establish direct interactions with RNA. To study this possibility, a recombinant histidine-tagged version of the IBDV VP3 was produced and purified. Purified VP3 was then used to perform a number of assays to unambiguously determine its ability to interact with different RNAs in the absence of other IBDV-encoded proteins. Since preliminary results indicated that VP3 bound ssRNA as well as dsRNA, ssRNA probes were used for subsequent RNA-binding analyses.

The histidine-tagged baculovirus-expressed VP3 protein interacts with ssRNA

In order to obtain sufficient purified VP3 to perform a series of biochemical experiments described below, VP3-Bac, a rBV, was generated. This virus expressed a N-terminal histidine-tagged version of VP3 under the control of the polyhedrin promoter. The ability of VP3 to bind ssRNA was initially tested by Northwestern blotting using total cell extracts from either WT baculovirus or VP3-Bac-infected cells. The assays were carried out using ^{32}P-labeled ssRNA probe B. This probe

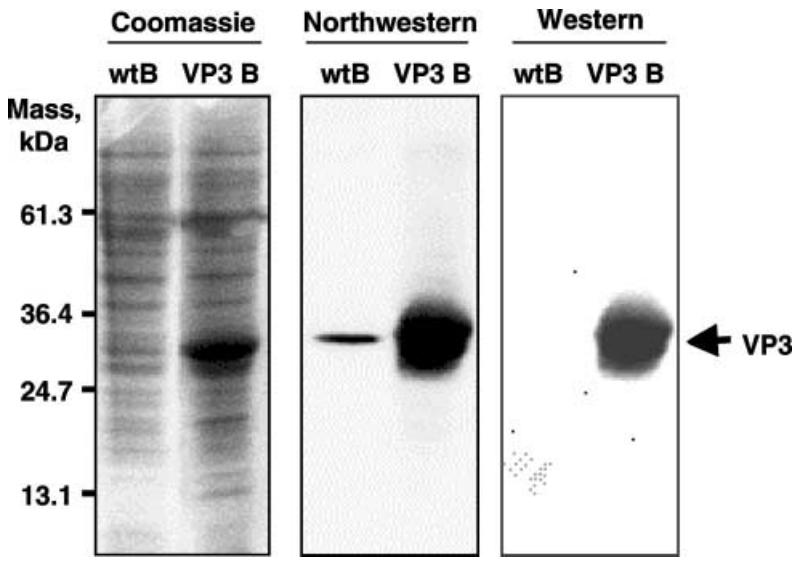

Fig. 1. Characterization of VP3 ssRNA-binding activity by Northwestern analysis. SDS-PAGE analysis of baculovirus-expressed recombinant VP3 (VP3 B) in insect cells and Coomassie staining, as indicated above the gel (left). Northwestern analysis of recombinant VP3 using radioactive labeled ssRNA probe B (center). Western-blot analysis using anti-VP3 specific MAb of the samples analyzed by Northwestern (right). *WTB*, cell extract from WT baculovirus-infected insect cells; *VP3 B*, cell extract from insect cells infected with rBV expressing VP3. The arrow indicates the position of the VP3 protein

was initially chosen since it contained the 5′ and 3′ UTRs from IBDV segment B, which might play an important role in virus replication and encapsidation. As revealed by SDS-PAGE and Coomassie staining of cell extracts (Fig. 1), VP3 was expressed at high levels in cells infected with VP3-Bac. A significant binding with ssRNA probe B was observed by the expressed VP3 in VP3-Bac infected cell extracts (Fig. 1). A weak but significant band of bound probe was observed also in WT-infected cells, at the same position as IBDV VP3. This band accounted for a 5% of total bound RNA probe when compared to the cell lysate containing VP3, as determined by densitometric analysis. Western blot analysis with a VP3-specific MAb confirmed that the RNA-binding protein expressed after infection with VP3-Bac was in fact VP3 protein (Fig. 1). The RNA-binding protein present in cells infected with WT baculovirus did not react with VP3-specific antibodies, suggesting that this protein was either cellular or viral, but not VP3. These results also showed that monomers of VP3 fixed to nitrocellulose filters bound the ssRNA probe B.

Characterization of the VP3 ssRNA-binding activity by EMSA

To further characterize the binding properties of purified VP3 to ssRNA, EMSA assays were performed with ^{32}P-labeled probe B. Purified VP3 was used for these

studies instead of total cellular extracts due to the existence of an RNA-binding protein in control cell extracts that might interfere with the results (Fig. 1). A series of shifted bands of RNA-protein complexes were visualized after incubation of purified VP3 with radioactive probe B (Fig. 2). The intensity of these bands was directly dependent upon the amount of VP3 used in the binding reaction mixtures (Fig. 2A), reaching a plateau above a VP3 concentration of 6×10^{-4} mM. Results were reproducibly observed in all experiments. No shifted bands were observed when relatively high amounts of BSA were used in the binding mixtures, as expected (Fig. 2). These results further showed that baculovirus-expressed VP3 bound ssRNA probe B. Since pure VP3 was used for the studies, these results also showed that VP3 did not require the presence of other virus or cellular proteins to bind ssRNA.

To confirm that the shifted bands corresponded to ribonucleoprotein complexes containing VP3 and not to aggregated RNA, supershift assays were performed using purified VP3 protein-specific MAbs (Fig. 2B). When BSA was used as a control at high amounts, no shifted bands were observed (Fig. 2B). In constrast, VP3 alone or in the presence of a non-specific IgG formed at least three ribonucleoprotein complexes of different electrophoretic mobilities (Fig. 2B). The complex of higher electrophoretic mobility probably corresponded to monomer VP3 molecules binding to the RNA probe, since when low amounts of VP3 protein were used in binding reactions this was the only shifted band (Fig. 2A). Addition of VP3 protein-specific MAbs caused the supershift of all the complexes (Fig. 2B). These results unambiguously confirmed that the shifted bands corresponded to ribonucleoprotein complexes containing VP3.

Estimation of VP3-ssRNA dissociation constant

After confirming that VP3 bound ssRNA probe B, VP3-RNA complex dissociation constant was estimated by binding ribonucleoprotein complexes to nitrocellulose filters, as described in Materials and Methods. The percentage of the retained radioactivity in nitrocellulose filters was represented as a function of VP3 concentration (Fig. 3A). A plateau of VP3-RNA binding was observed at VP3 concentrations above 10^{-4} mM. The VP3-RNA dissociation constant was derived from binding curves, and it was estimated from 3 independent experiments to be of $2 \pm 0.2 \times 10^{-4}$ mM ($n = 3$; Spearman's coefficient of variation, $CV = 10\%$). Similar results were obtained with different ssRNA probes (data not shown). A Hill plot for the binding of VP3 to ssRNA was derived (Fig. 3B), calculating a regression line with a correlation coefficient ($R = 0.9705$; 9 degrees of freedom; $t = 12.07$) – associated probability (P) of 9.97×10^{-5}, showing a very significant correlation of data to a linear relationship. The Hill coefficient (n_H) derived from the regression line was 0.97 (Fig. 3B), slightly lower than 1, showing that VP3 bound ssRNA in a non-cooperative manner. The $K_{0.5}$ was calculated from the regression line, giving a result of 1.02×10^{-4} mM, close to the estimated apparent Kd (Fig. 3B).

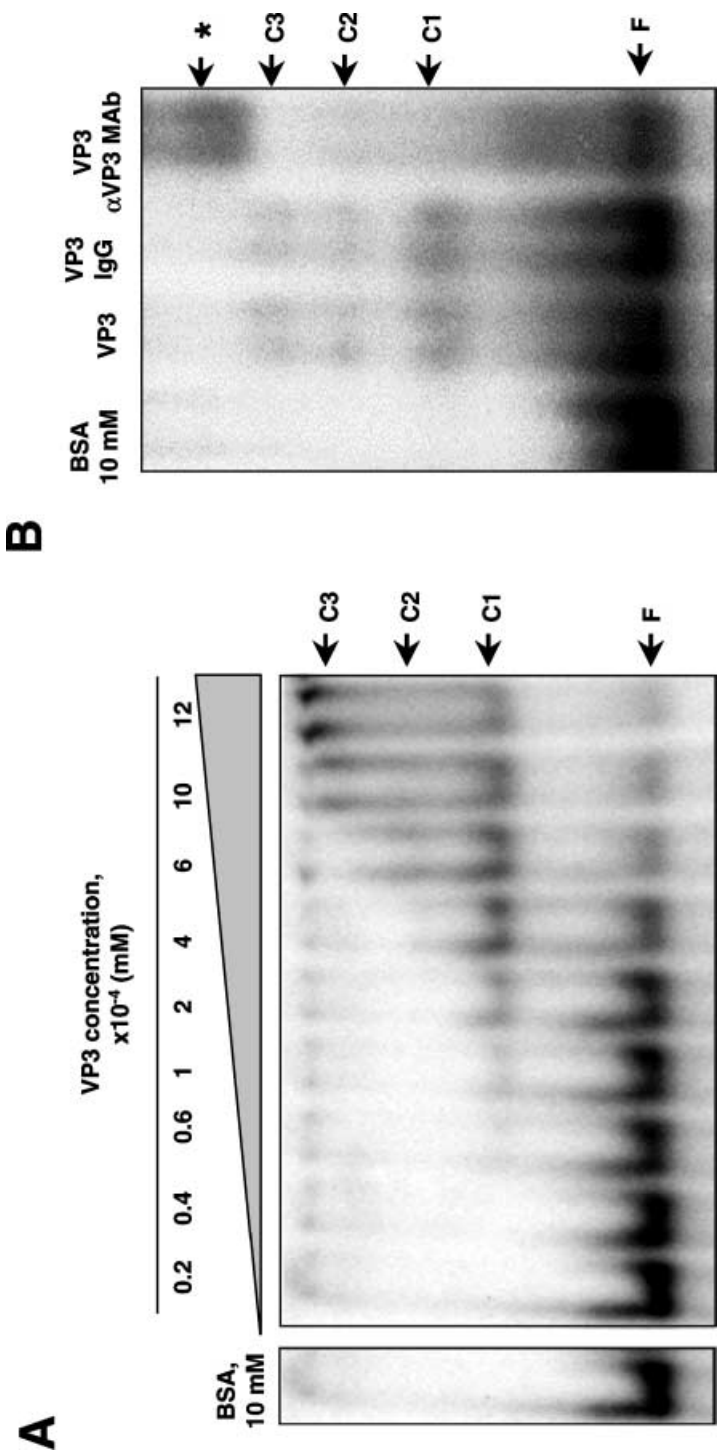

Fig. 2. Characterization of the VP3 ssRNA-binding activity by EMSA. **A** Native polyacrylamide electroforesis gel of VP3 and radioactive ssRNA probe B complexes. Increasing concentrations of VP3 were used, as indicated above the gel. Excess BSA was used as nonspecific control protein. **B** Native polyacrylamide electroforesis gel of VP3 and radioactive ssRNA probe B complexes in the absence (*VP3*) or presence of nonspecific IgG (*VP3 IgG*) or VP3-specific MAb (*VP3 αVP3 MAb*). *F*, free RNA probe B; *C1*, *C2* and *C3*, VP3-RNA complexes of higher, middle and lower electrophoretic mobilities; *, supershifted VP3-RNA-MAb complexes

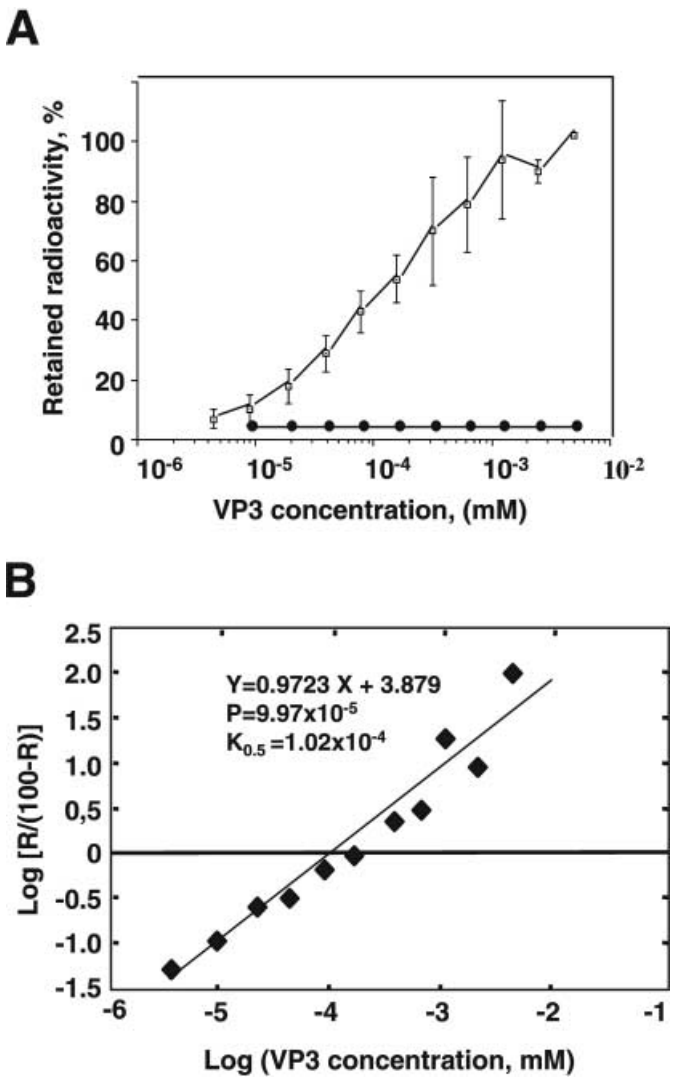

Fig. 3. Determination of VP3 ssRNA-binding dissociation constant and Hill coefficient. **A** The graph represents the retained radioactivity in nitrocellulose filters as a function of protein concentration, after formation of VP3 and radioactive ssRNA probe B complexes. Increasing concentrations of purified VP3 (□) or BSA (●) were used in the assays. Means from three independent experiments are represented, together with error bars. **B** A Hill plot of VP3 binding to ssRNA is represented and the calculated regression line is shown. The regression line equation and the associated regression probability (*P*) are shown above the line; $K_{0.5}$, VP3 concentration in which the regression line cuts the Y axis (concentration in which half saturation is reached, or apparent Kd); *R*, percentage of retained radioactivity

Characterization of the specificity of VP3-ssRNA interaction

The experiments described above were performed using probe B that contained the 5′ and 3′ UTRs from IBDV genome segment B. Competition experiments were performed to find out whether the VP3-RNA interaction was sequence-specific.

For this, increasing concentrations of different unlabeled RNA or DNA competitor probes were included in the VP3/RNA reaction mixtures. After incubation, samples were filtered though nitrocellulose membranes, and the amount of retained radioactivity estimated. As expected, binding of VP3 to labeled ssRNA probe B was efficiently competed by the addition of unlabeled probe B (Fig. 4A). A similar result was obtained when ssRNA probe A was used (Fig. 4B). Nonviral ssRNA

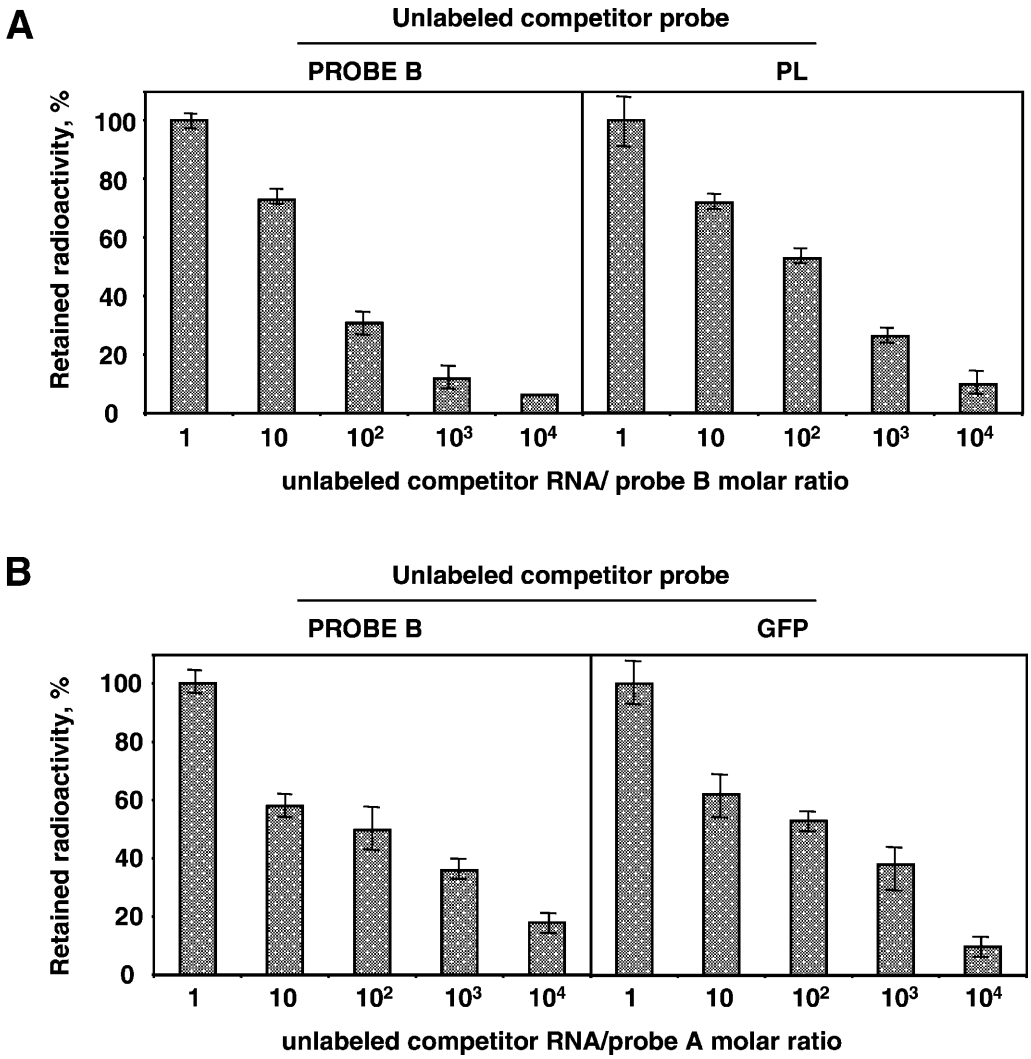

Fig. 4. Inhibition of VP3 binding to labeled ssRNA probes by unlabeled competitor RNAs. **A** Graphs represent the percentage of retained radiactivity in nitrocellulose membranes from complexes formed by VP3 and labeled ssRNA probe B, as a function of the ratios of unlabeled ssRNA probes B (left graph) or PL (right graph) to labeled probe B. Data is represented as the mean of three independent experiments together with error bars. **B** Graphs represent the percentage of retained radiactivity in nitrocellulose membranes from complexes formed by VP3 and labeled ssRNA probe A, as a function of the ratio of unlabeled ssRNA probes A (left graph) or GFP (right graph) to labeled probe A

probes PL and GFP also competed with probes B and A, respectively (Fig. 4A and B), indicating that VP3 binding to ssRNA was sequence-independent. IBDV contains a dsRNA genome probably in close contact with VP3 molecules in IBDV virions [6, 9]. To find out whether VP3 presented a binding activity to IBDV dsRNA, competition experiments using purified IBDV dsRNA were performed. As shown in Fig. 5, IBDV purified dsRNA segment A efficiently competed the binding of VP3 to labeled ssRNA probe A. This also suggested that VP3 probably bound ssRNA and dsRNA through the same interaction domain. Interestingly, dsDNA did not significantly compete the binding (Fig. 5). Single-stranded DNA efficiently competed with the binding of VP3 to probe A, showing that VP3 also bound ssDNA (Fig. 5).

Mapping of the VP3 ssRNA-binding domain

In order to identify the VP3 protein region involved in ssRNA-binding, a set of mutants with deletions of about 20 aa covering the whole protein was generated (Fig. 6A). VP3 deletion mutants were expressed and purified as described in Materials and Methods. After purification, proteins were analyzed and quantified by SDS-PAGE and Coomassie staining (Fig. 6B). Interestingly, except for the VP3Δ971–1012 deletion mutant, the samples contained two VP3 electrophoretic forms, resulting in doublets in SDS-PAGE gels (Fig. 6B). Bands corresponding to higher molecular mass species migrated according to their expected molecular masses. Estimation of the molecular masses of the lower protein bands indicated a consistent reduction of about 1.5 kDa compared to the expected size (Fig. 6B).

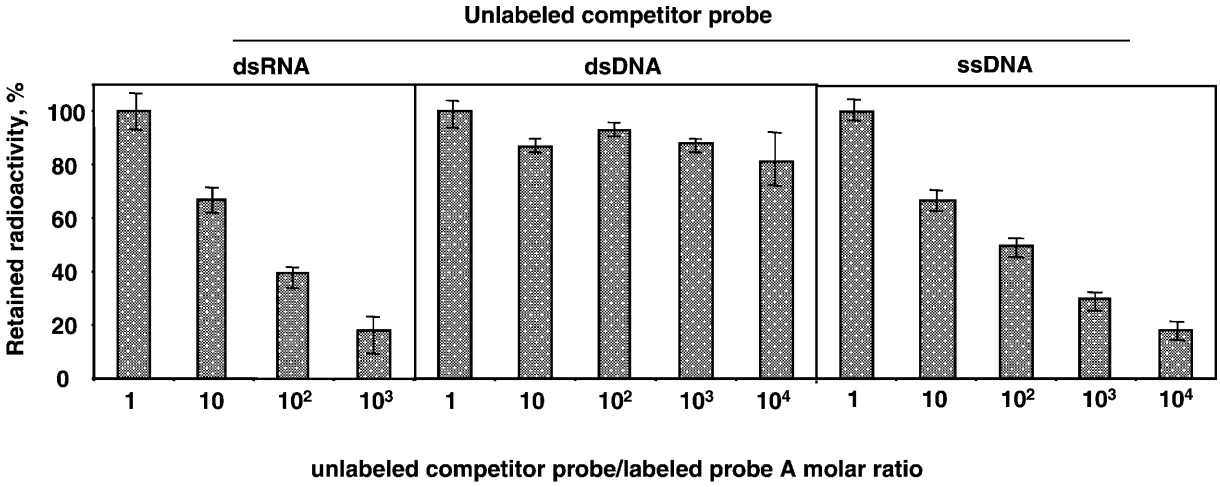

Fig. 5. Characterization of VP3-dsRNA binding by competition experiments. Graphs represent the percentage of retained radiactivity in nitrocellulose membranes from complexes formed by VP3 and labeled ssRNA probe A, as a function of the ratios between unlabeled dsRNA genome segment A (left graph), ds plasmid DNA (central graph) or ssDNA (right graph) to labeled probe A. Data is represented as means from three independent experiments with error bars

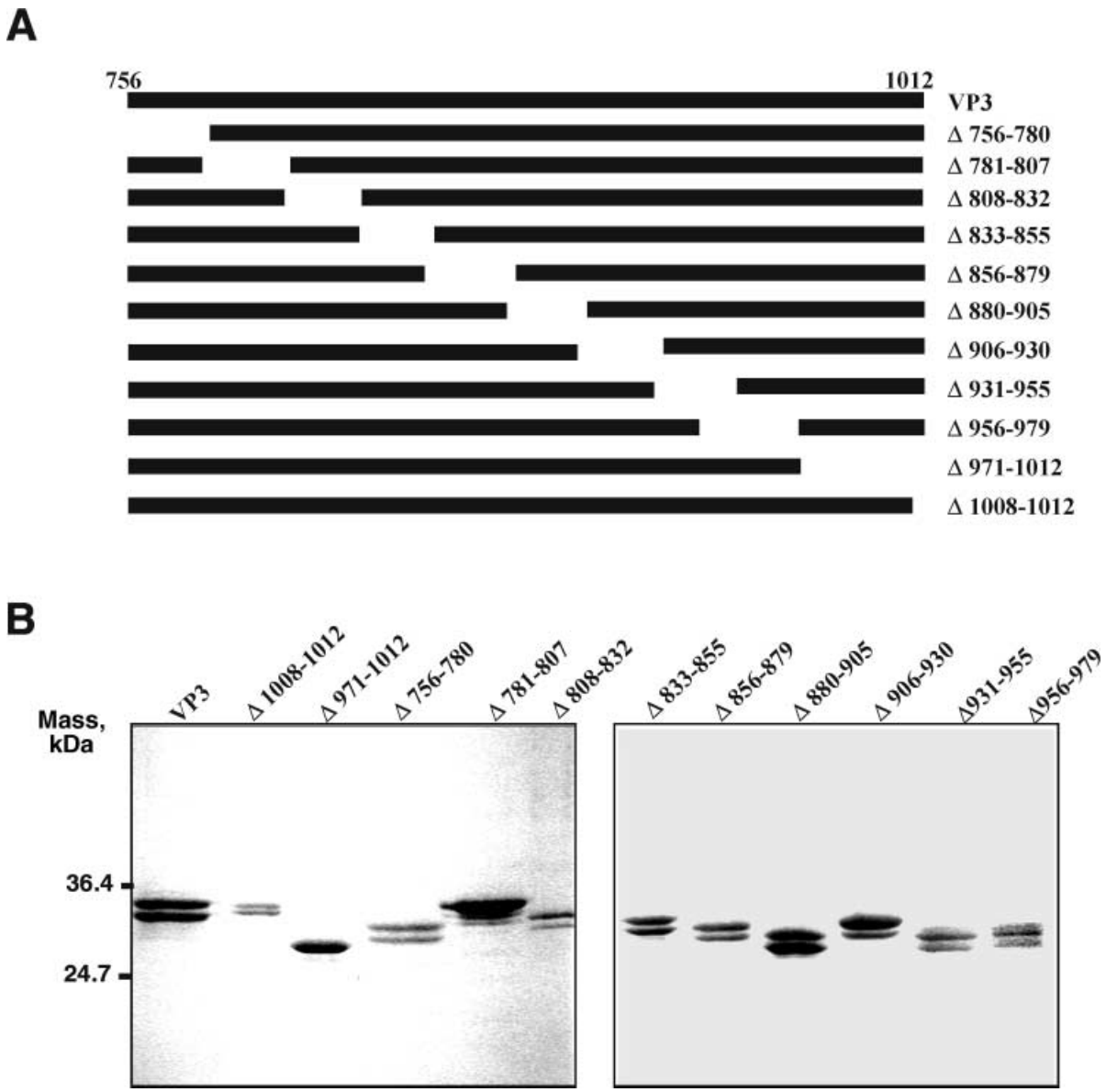

Fig. 6. Expression and purification of VP3 deletion mutants. **A** Set of deletions introduced throughout the VP3 protein sequence from the amino-terminus to the carboxy-terminus. Numbers indicate aminoacid positions from the polyprotein sequence. Mutants are named according to the positions in which deletions are inserted. **B** SDS-PAGE analysis and Coomassie staining of purified VP3 deletion mutants as indicated above the gels

Northwestern analyses showed that both wild-type-derived VP3 forms interacted with labeled ssRNA probes (data not shown).

The affinity of each mutant protein to ssRNA was determined by membrane filter binding assays, using probe B, as described above. The amounts of the purified deletion mutant proteins used in these assays were normalized according to their respective molecular masses. Identical molar amounts of each mutant

protein were used in the assays. The ssRNA-binding activity of WT VP3 was estimated to have an apparent Kd of $(2 \pm 0.2) \times 10^{-4}$ mM (n = 3, CV = 10%) (Figs. 3 and 7). Deletion mutants VP3Δ756–780 and VP3Δ781–807 presented a slightly reduced affinity compared to that of WT VP3. Carboxy-terminal deletion mutants showed an affinity similar to that of the complete VP3 protein, indicating that the ssRNA-binding domain was not affected by these deletions (Fig. 7). In contrast, mutants presenting deletions at the region between residues 808 and 879 showed significantly lower affinities to ssRNA, up to 100-fold reduction in

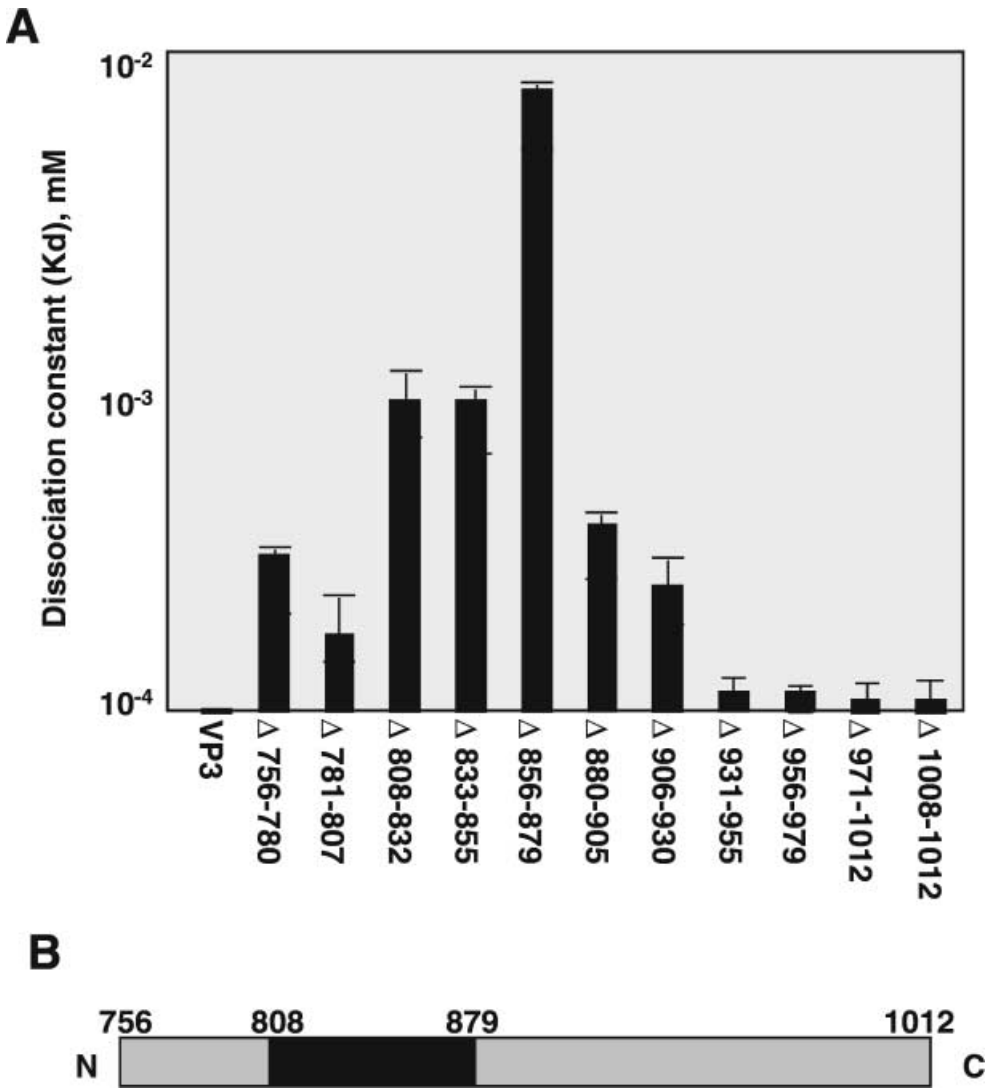

Fig. 7. Identification of the VP3 ssRNA-binding domain. **A** Graph representing the estimated dissociation constant for each of the purified VP3 deletion mutants shown in Fig. 6. Means from three independent experiments are represented with error bars. **B** Scheme representing the VP3 protein. The identified ssRNA interaction domain is represented as a black box. Numbers indicate positions in the polyprotein

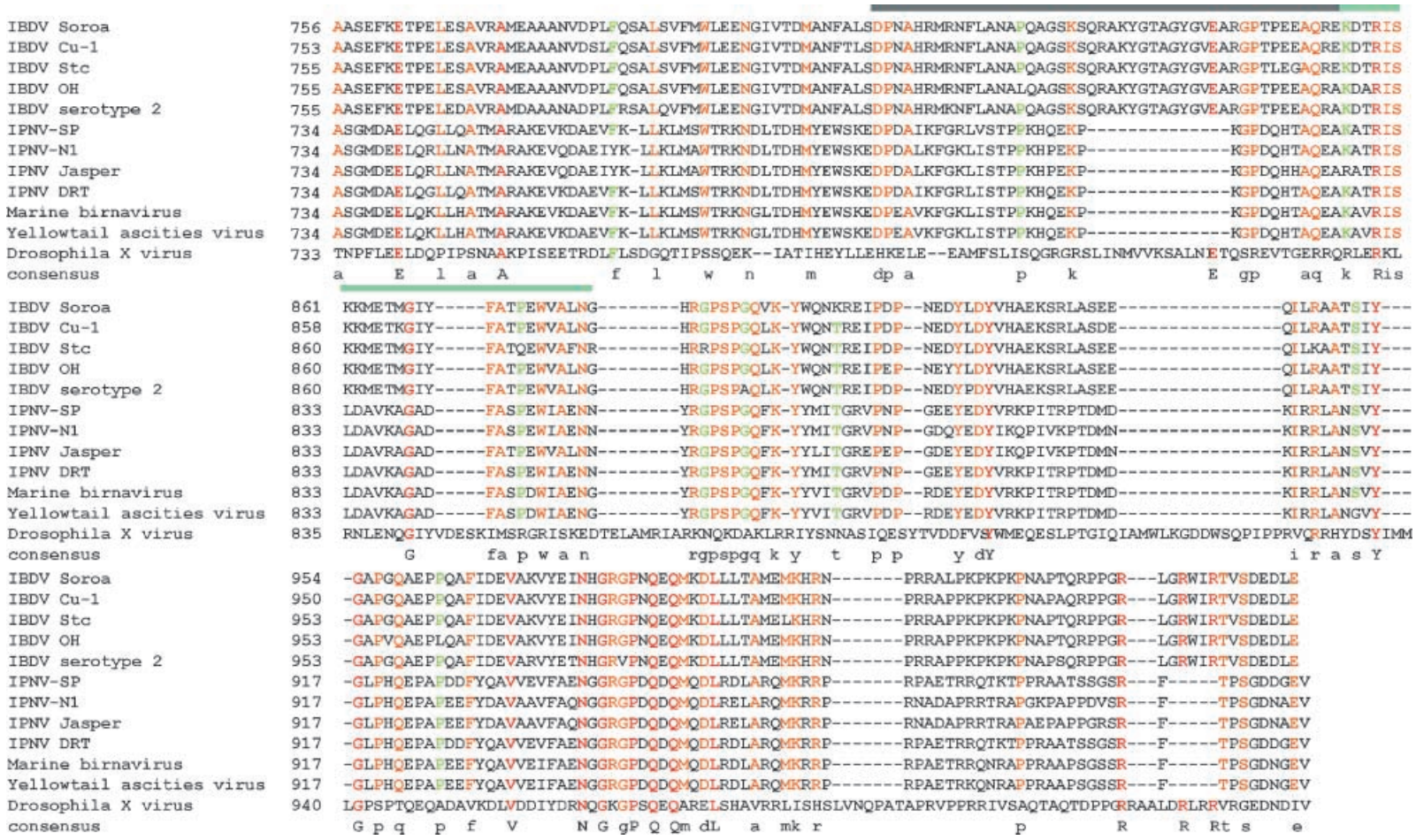

Fig. 8. Sequence comparison of VP3 proteins from species belonging to the family *Birnaviridae*. An alignment of VP3 protein sequences from the indicated virus species and the VP3 consensus sequences are shown. A bar is placed above the region involved in ssRNA binding. The green bar indicates the most sensitive region to deletions that abrogate VP3-ssRNA binding. Residues in red indicate totally conserved aminoacids. In orange, highly conserved residues are indicated. Conservative aminoacid substitutions are shown in green. VP3 residues are numbered according to polyprotein positions

the case of VP3Δ856–879 deletion mutant. These results indicated that the VP3 ssRNA-binding domain was located within a region comprising from residues 808 to 879 (Fig. 7B).

Sequence conservation of the VP3 ssRNA-binding domain

To investigate whether the identified ssRNA-binding domain presented highly conserved sequence features, a comparison was performed using the polyprotein sequences of representative species from the family *Birnaviridae*. The alignment and comparison of VP3 protein sequences revealed that in the region implicated in RNA-binding, strains from the genus *Avibirnavirus* contained a 14 aa sequence absent in their counterparts from the aquabirnavirus genus (Fig. 8). In addition, sequence comparisons showed two absolutely conserved residues, Arg_{858} and Gly_{867}, within this region. A highly hydrophobic region, including the conserved Gly_{867} (G–FA-P-W-A-N) was also found between residues 867 and 879 (Fig. 8). Interestingly, when this region was deleted from VP3 (VP3Δ856–879), the ssRNA-binding activity was most severely impaired (Fig. 7), suggesting that this region might play a critical role for ssRNA-binding. Other highly conserved short sequences were also found, but RNA or DNA binding motifs previously described in the literature such as zinc fingers, arginine-rich regions or RG boxes, were not found within VP3 [8]. Whether this region contains a previously unpublished RNA-binding motif, or if it comprises a double-stranded RNA-binding motif [8] is currently under investigation. A detailed mutagenesis study is being carried out to identify which of the conserved regions in the RNA-binding domain is directly involved in RNA-binding.

Discussion

Capsids of dsRNA viruses having a life cycle including an extracellular phase contain two or more protein layers [2, 9]. Strikingly, capsids of members of the *Birnaviridae* family are much simpler. They contain a single protein shell [6, 9]. This unique feature makes especially interesting the study of both the molecular architecture and the morphogenesis of birnaviruses. The inner surface of the IBDV particle is coated by 200 Y-shaped VP3 trimers in close contact with the continuous shell formed by VP2 [6, 9]. Although the precise capsid location of the putative RdRp, VP1, has not been established yet, it has been shown that it directly interacts with VP3 [28, 43]. Therefore, VP3 appears to play a crucial structural role. It has been suggested that VP3 might interact with the dsRNA genome segments [9, 22, 23]. Indeed, its presence in ribonucleoprotein complexes isolated from disrupted IPNV virions [22], makes it a good candidate for playing a role in genome packaging and/or stabilization. It was therefore interesting to analyze the ability of VP3 to interact with RNA. We decided to undertake this analysis using a histidine-tagged version of the protein produced in insect cells infected with rBVs. The protein obtained under these conditions was highly pure and soluble, thus enabling us to carry out a number of highly specific assays.

rBV-expressed VP3 exhibited a ssRNA-binding activity as determined by Northwestern and EMSA assays. However, extracts from cells infected with wild-type baculovirus also contained an RNA-binding protein. The presence of this either cellular or viral protein prevented further studies on the VP3 RNA-binding properties, especially for Kd estimations. For this reason further studies were carried out with affinity-purified VP3.

VP3 presented a ssRNA-binding activity with an approximate Kd of $(2 \pm 0.2) \times 10^{-4}$ mM as directly determined from VP3-RNA binding curves. VP3-RNA binding curves were also represented as a Hill plot, in order to calculate Kd and the Hill coefficient. The calculated n_H (0.97) for VP3-ssRNA binding was slightly lower than 1. However, it really cannot be considered as negative cooperativity, but rather as non-cooperative binding. An alternative derivation of Kd by calculating $K_{0.5}$ in the Hill plot also agreed with the estimated Kd for VP3-ssRNA binding. This Kd value falls within the range of other viral and cellular nucleic acid-binding proteins [31, 38, 42].

Interestingly, the EMSA assays revealed at least three VP3-ssRNA complexes with different electrophoretic mobilities. Two possibilities could explain the presence of the multiple shifted bands observed: i) VP3 could contain more than one RNA-binding domain; and ii) VP3 could form oligomers that bind RNA. The most abundant complex corresponded to the faster migrating band, even when extremely low concentrations of VP3 were used in the assays. This observation suggested that most likely the faster migrating band was formed by VP3 monomers. Moreover, the binding of VP3 to ssRNA in Northwestern assays showed that VP3 monomers generated under denaturing conditions bound ssRNA. The ability of VP3 to form oligomers has been assessed using a two-hybrid system approach [43], and the structural analyses of IBDV particles and VLPs have revealed that VP3 molecules form trimers in the internal surface of the capsid [9]. Therefore, it is likely that VP3 might also form trimers under the conditions used for RNA-binding studies, explaining the presence of lower mobility shift bands when VP3 concentration was increased. However, the ability of recombinant VP3 to form trimers has not been tested in this work.

Competition experiments revealed that VP3 bound ssRNA in a sequence-independent manner. The lack of any binding specificity to ssRNA probes used in this study might indicate that, as it is the case with other virus-encoded nucleoproteins [20, 26, 33, 42], other factor(s) could be necessary to confer specificity. VP1, the putative IBDV RdRp, is the most likely candidate for this role.

Interestingly, VP3 bound dsRNA and ssDNA, apparently through the same ssRNA-binding domain, but not dsDNA. These binding characteristics are usually found in RNA-binding proteins, especially in dsRNA-binding proteins [14]. The ability of VP3 to interact with ssRNA and dsRNA could reflect the possibility that genome replication and transcription, assumed to be carried out by VP1, could be assisted by VP3 binding both to IBDV ssRNA and dsRNA.

In order to identify the VP3 protein domain involved in RNA-binding, a series of deletion mutants were expressed and purified. Interestingly, two protein forms were observed for each mutant, except for VP3Δ971–1012. This is consistent

with a proteolytic processing at the VP3 carboxy terminus, since VP3Δ971–1012 deletion mutant lacking the 41 C-terminal residues only presented a single band of the expected molecular mass (Fig. 6). VP3 presents two electrophoretic forms in IBDV-infected cells. VP3 doublets have been described in previous reports. However the nature and function of these forms remain unknown [43]. Interestingly, only the full length VP3 protein is incorporated in IBDV virions, suggesting that the shorter form might have additional, non-structural, functions. It could also be possible that cellular proteases such as caspases [15] could be involved in VP3 processing. Alternatively, VP3 could exhibit an autoproteolytic activity not previously reported.

The Kd for each VP3 deletion mutant was determined, and it was found that deletions affecting to the VP3 region between residues 808 to 879 abrogated VP3 ssRNA-binding activity. The loss of ssRNA-binding activity exhibited by these VP3 deletion mutants was not due to loss of protein solubility, since in all experiments VP3 mutants were soluble. Although deletions could affect the VP3 structure, this is unlikely. Small deletions were introduced to avoid dramatic changes in protein structure. Additionally, only deletions between residues 808 and 879 did have an effect on ssRNA-binding activity, while the rest of the mutants efficiently bound ssRNA. Interestingly, ssRNA-binding was severely impaired by the deletion of a short, highly conserved sequence between residues 856–879. Whether this region is directly involved in binding to ssRNA and dsRNA, is a subject of investigation.

To our knowledge, this is the first time that an RNA-binding activity has been demonstrated for a birnavirus VP3 protein. VP3 protein bound ssRNA and dsRNA, exhibiting no specificity for virus-derived ssRNA probes. The identification of critical residues for RNA-binding activity within VP3 RNA-binding domain is currently under investigation. The implications of VP3 RNA-binding activity are also being investigated in the context of the virus replication and transcription.

Acknowledgements

We are grateful to J. Castón and A. Maraver for critical reading of the manuscript; to S. Gonzalez and P. Gastaminza for interesting and helpful discussion; to H. Müller for anti-VP3 monoclonal antibodies; A. Maraver for plasmid TV2-5′3′; to E. Camafeita for protein analyses.

This work was supported by grants BIO-97-0576 from the Comisión Interministerial de Ciencia y Tecnología, 07B/0032/1998 from the Subdirección General de Investigación of the Comunidad Autónoma de Madrid.

References

1. Bachurski CJ, Kelly SE, Glasser SW, Currier TA (1997) Nuclear factor I family members regulate the transcription of surfactant protein-C. J Biol Chem 272: 32759–32766
2. Baker TS, Olson NH, Fuller SD (1999) Adding the third dimension to virus life cycles: three-dimensional reconstructions of icosaedral viruses from cryoelectron micrographs. Microbiol Mol Biol Rev 63: 862–922

3. Bardsley WG, Woolfson R, Mazat JP (1980) Relationships between the magnitude of Hill plot slopes, apparent binding constants and factorability of bindings polynomials and their Hessians. J Theor Biol 85: 247–284
4. Birghan C, Mundt E, Gorbalenya AE (2000) A non-canonical lon proteinase lacking the ATPase domain employs the ser-Lys catalytic dyad to exercise broad control over the life cycle of a double-stranded RNA virus. EMBO J 19: 114–123
5. Black DL, Chan R, Min HH, Wang J, Bell L (1998) The electrophoretic mobility shift assay for RNA-binding proteins. In: Smith CWJ (ed) RNA-protein interaction. Oxford University Press, Oxford, pp 109–135
6. Bottcher B, Kiselev NA, Stel'Mashchuk VY, Perevozchikova NA, Borisov AV, Crowther RA (1997) Three-dimensional structure of infectious bursal disease virus determined by electron cryomicroscopy. J Virol 71: 325–330
7. Bruenn JA (1991) Relationships among the positive strand and double-strand RNA viruses as viewed through their RNA-dependent RNA polymerases. Nucleic Acids Res 19: 217–226
8. Burd CG, Dreyfuss G (1994) Conserved structures and diversity of functions of RNA-binding proteins. Science 265: 615–621
9. Caston JR, Martinez-Torrecuadrada JL, Maraver A, Lombardo E, Rodriguez JF, Casal JI, Carrascosa JL (2001) C terminus of infectious bursal disease virus major capsid protein VP2 is involved in definition of the T number for capsid assembly. J Virol 75: 10815–10828
10. Chevalier C, Lepault J, Erk I, Da Costa B, Delmas B (2002) The maturation process of pVP2 requires assembly of infectious bursal disease virus capsids. J Virol 76: 2384–2392
11. Da Costa B, Chevalier C, Henry C, Huet JC, Petit S, Lepault J, Boot H, Delmas B (2002) The capsid of infectious bursal disease virus contains several small peptides arising from the maturation process of pVP2. J Virol 76: 2393–2402
12. Dayhoff MO, Schwartz RM, Orcutt BC (1978) A model of evolutionary change in proteins, matrixes for detecting distant relationships. In: Dayhoff MO (ed) Atlas of protein sequence and structure, vol 5. National Biomedical Research Foundation, Washington, D.C., pp 345–358
13. Dobos P, Hill BJ, Hallett R, Kells DT, Becht H, Teninges D (1979) Biophysical and biochemical characterization of five animal viruses with bisegmented double-stranded RNA genomes. J Virol 32: 593–605
14. Draper DE (1999) Themes in RNA-protein recognition. J Mol Biol 293: 255–270
15. Eleouet JF, Slee EA, Saurini F, Castagne N, Poncet D, Garrido C, Solary E, Martin SJ (2000) The viral nucleocapsid protein of transmissible gastroenteritis coronavirus (TGEV) is cleaved by caspase-6 and -7 during TGEV-induced apoptosis. J Virol 74: 3975–3983
16. Fernandez-Arias A, Martinez S, Rodriguez JF (1997) The major antigenic protein of infectious bursal disease virus, VP2, is an apoptotic inducer. J Virol 71: 8014–8018
17. Fernandez-Arias A, Risco C, Martinez S, Albar JP, Rodriguez JF (1998) Expression of ORF A1 of infectious bursal disease virus results in the formation of virus-like particles. J Gen Virol 79: 1047–1054
18. Gardner H, Kerry K, Riddle M, Brouwer S, Gleeson L (1997) Poultry virus infection in Antarctic penguins. Nature 387: 245
19. Gonzalez S, Ortin J (1999) Characterization of influenza virus PB1 protein binding to viral RNA: two separate regions of the protein contribute to the interaction domain. J Virol 73: 631–637

20. Gott P, Stohwasser R, Schnitzler P, Darai G, Bautz EK (1993) RNA binding of recombinant nucleocapsid proteins of hantaviruses. Virology 194: 332–337
21. Hall AB, Kranz JK (1999) Nitrocellulose filter binding for determination of dissociation constants. In: Haynes S (ed) Methods in molecular biology, vol 118. Humana Press, Totowa, NJ, 105–128
22. Hjalmarsson A, Carlemalm E, Everitt E (1999) Infectious pancreatic necrosis virus: identification of a VP3- containing ribonucleoprotein core structure and evidence for O-linked glycosylation of the capsid protein VP2. J Virol 73: 3484–3490
23. Hjalmarsson A, Everitt E (1999) Identification of IPNV-specified components released from productively infected RTG-2 cells following massive cytopathic effect. Arch Virol 144: 1487–1501
24. Hudson PJ, McKern NM, Power BE, Azad AA (1986) Genomic structure of the large RNA segment of infectious bursal disease virus. Nucleic Acids Res 14: 5001–5012
25. Kibenge FS, Dhama V (1997) Evidence that virion-associated VP1 of *Avibirnaviruses* contains viral RNA sequences. Arch Virol 142: 1227–1236
26. Klein M, Eggers HJ, Nelsen-Salz B (2000) Echovirus-9 protein 2C binds single-stranded RNA unspecifically. J Gen Virol 81: 2481–2484
27. Leong JC, Brown D, Dobos P, Kilbenge FSB, Ludert JE, Muller H, Nicholson B (2000) Family *Birnaviridae*. In: Van Regenmortel MHV, Faquet CM, Bishop DHL, Carstens EB, Estes MK, Lemon SM, Maniloff J, Mayo MA, McGeoch DJ, Pringle CR and Wickner RB (eds) Virus Taxonomy, Seventh Report of International Committee on Taxonomy of Viruses. Academic Press, San Diego, pp 481–490
28. Lombardo E, Maraver A, Caston JR, Rivera J, Fernandez-Arias A, Serrano A, Carrascosa JL, Rodriguez JF (1999) VP1, the putative RNA-dependent RNA polymerase of infectious bursal disease virus, forms complexes with the capsid protein VP3, leading to efficient encapsidation into virus-like particles. J Virol 73: 6973–6983
29. Lombardo E, Maraver A, Espinosa I, Fernandez-Arias A, Rodriguez JF (2000) VP5, the nonstructural polypeptide of infectious bursal disease virus, accumulates within the host plasma membrane and induces cell lysis. Virology 277: 345–357
30. Macreadie IG, Azad AA (1993) Expression and RNA dependent RNA polymerase activity of birnavirus VP1 protein in bacteria and yeast. Biochem Mol Biol Int 30: 1169–1178
31. Marcos JF, Vilar M, Perez-Paya E, Pallas V (1999) *In vivo* detection, RNA-binding properties and characterization of the RNA-binding domain of the p7 putative movement protein from carnation mottle carmovirus (CarMV). Virology 255: 354–365
32. Muller H, Nitschke R (1987) The two segments of the infectious bursal disease virus genome are circularized by a 90,000-Da protein. Virology 159: 174–177
33. Muriaux D, Mirro J, Harvin D, Rein A (2001) RNA is a structural element in retrovirus particles. Proc Natl Acad Sci U S A 98: 5246–5251
34. Nagarajan MM, Kibenge FS (1997) Infectious bursal disease virus: a review of molecular basis for variations in antigenicity and virulence. Can J Vet Res 61: 81–88
35. Ogawa M, Wakuda T, Yamaguchi T, Murata K, Setiyono A, Fukushi H, Hirai K (1998) Seroprevalence of infectious bursal disease virus in free-living wild birds in Japan. J Vet Med Sci 60: 1277–1279
36. Pogulis RJ, Vallejo AN, Pease LR (1996) *In vitro* recombination and mutagenesis by overlap extension PCR. Methods Mol Biol 57: 167–176
37. Press WH, Flannery BP, Teukolsky SA, Vetterling WT (1992) Linear correlation. In: Numerical recipes in FORTRAN: the art of scientific computing. Cambridge University Press, Cambrigde, 630–633

38. Purohit P, Dupont S, Stevenson M, Green MR (2001) Sequence-specific interaction between HIV-1 matrix protein and viral genomic RNA revealed by *in vitro* genetic selection. RNA 7: 576–584
39. Saif YM (1998) Infectious bursal disease and hemorrhagic enteritis. Poult Sci 77: 1186–1189
40. Sanchez AB, Rodriguez JF (1999) Proteolytic processing in infectious bursal disease virus: identification of the polyprotein cleavage sites by site-directed mutagenesis. Virology 262: 190–199
41. Schuler GD (1998) Sequence alignment and database searching. In: Baxevanis AD, Quellette BFF (eds) Bioinformatics: a practical guide to the analysis of genes and proteins. Wiley-Liss, Inc., New York, 145–171
42. Skuzeski JM, Morris TJ (1995) Quantitative analysis of the binding of turnip crinkle virus coat protein to RNA fails to demonstrate binding specificity but reveals a highly cooperative assembly interaction. Virology 210: 82–90
43. Tacken MG, Rottier PJ, Gielkens AL, Peeters BP (2000) Interactions *in vivo* between the proteins of infectious bursal disease virus: capsid protein VP3 interacts with the RNA-dependent RNA polymerase, VP1. J Gen Virol 81: 209–218
44. Ward GA, Stover CK, Moss B, Fuerst TR (1995) Stringent chemical and thermal regulation of recombinant gene expression by vaccinia virus vectors in mammalian cells. Proc Natl Acad Sci U S A 92: 6773–6777
45. Wilcox GE, Flower RL, Baxendale W, Smith VW (1983) Infectious bursal disease in Western Australia. Aust Vet J 60: 86–87
46. Yao K, Vakharia VN (2001) Induction of apoptosis *in vitro* by the 17-kDa nonstructural protein of infectious bursal disease virus: possible role in viral pathogenesis. Virology 285: 50–58

Author's address: S. L. Bionostra, Ronda de Poniente 4, Tres Cantos E-28760 Madrid, Spain; e-mail: grazynak@bionostra.com